Hindawi
Wireless Communications and Mobile Computing
Volume 2021, Article ID 2036778, 12 pages
https://doi.org/10.1155/2021/2036778

Research Article

Improving Performance of User Pair Using Reconfigurable Intelligent Surfaces

Kaveti UmaMaheswari,[1] **Arjun Chakravarthi Pogaku**,[1] **Dinh-Thuan Do**,[1] **Anh-Tu Le**,[2] **and Munyaradzi Munochiveyi**[3]

[1]*Department of Computer Science and Information Engineering, College of Information and Electrical Engineering, Asia University, Taichung 41354, Taiwan*
[2]*Faculty of Electronics Technology, Industrial University of Ho Chi Minh City (IUH), Ho Chi Minh City 700000, Vietnam*
[3]*Electrical and Electronics Engineering Department, University of Zimbabwe, Mount Pleasant, Harare, Zimbabwe*

Correspondence should be addressed to Munyaradzi Munochiveyi; mmunochiveyi@eng.uz.ac.zw

Received 13 August 2021; Accepted 25 November 2021; Published 23 December 2021

Academic Editor: Vinayakumar Ravi

With the given scope for new use cases and the demanding needs of future 6th generation (6G) wireless networks, the development of wireless communications looks exciting. The propagation medium has been viewed as a randomly behaving entity between the transmitter and the receiver since traditional wireless technology, degrading the quality of the received signal due to the unpredictable interactions of the broadcast radio waves with the surrounding objects. On the other hand, network operators could now manipulate electromagnetic radiation to remove the negative impacts of natural wireless propagation due to the recent arrival of reconfigurable intelligent surfaces (RIS) in wireless communications. According to recent findings, the RIS mechanism benefits nonorthogonal multiple access (NOMA), which can effectively deliver effective transmissions. For simple design, of RIS-NOMA system, fixed power allocation scheme for NOMA is required. The main system performance metric, i.e., outage probability, needs to be considered to look at the efficiency and capability of transmission mode relying on RIS and NOMA schemes, motivated by the potential of these developing technologies. As major performance metrics, we derive analytical representations of outage probability, and throughput and an accurate approximation is obtained for the outage probability. Numerical results are conducted to validate the exactness of the theoretical analysis. It is found that increasing the higher number of reflecting elements in the RIS can significantly boost the outage probability performance, and the scenario with only the RIS link is also beneficial. In addition, it is desirable to deploy the RIS-NOMA since it is indicated that better performance compared with the traditional multiple access technique.

1. Introduction

Due to high demands in terms of system capacity and spectrum efficiency, the traditional orthogonal multiple access (OMA) has been unable to meet the user needs to be associated with the rapid growth of Internet of Things (IoT) and mobile communications [1–7]. To meet the heavy demand for mobile services, nonorthogonal multiple access (NOMA) is researched in recent years with promising applications [8, 9]. In some scenarios, NOMA benefits to device-to-device communications [10, 11] and cognitive radio- (CR-) aided NOMA [12–14], and these are considered as potential key technologies for the fifth-generation mobile communications (5G). The authors in [13] deployed the relaying scheme for the secondary network of the considered CR-NOMA, and the relay can energy harvesting (EH) from the secondary transmitter to serve signal forwarding to distant secondary users. They studied the complex model of EH-assisted CR-NOMA in terms of outage behavior and throughput performance when has imperfect successive interference cancellation (SIC). Reference [14] presented relay-aided CR-NOMA networks to improve the performance of far users by enabling partial relay selection architecture. They explored system performance in terms of full-duplex (FD)

and half-duplex (HD) relays for both uplink and downlink communications.

Recently, due to its high-energy efficiency, reconfigurable intelligent surface (RIS) technique is recognized as the next-generation relay technique, also namely relay 2.0 [15–17]. The RIS elements can independently shift the signal phase and absorbing the signal energy. The reflected signals benefit to wireless transmission due to less energy required [18–25]. In [21], the authors demonstrated an interesting RIS architecture which includes any number of passive reflecting elements, a simple controller for their adjustable configuration, and a single radio frequency (RF) chain for baseband measurements. By assuming sparse wireless channels in the beam space domain, they studied an alternating optimization scheme for explicit estimation of the channel gains at the RIS elements attached to the single RF chain [21]. The authors in [22] explored RIS by combining the functions of phase shift and radiation together on an electromagnetic surface. As such, positive intrinsic-negative (PIN) diodes are employed to realize 2-bit phase shifting for beam forming. Thanks to providing RIS equipped 256 two-bit elements, this radical design is recognized as first wireless communication prototype in the world. The developed prototype includes main components such as modular hardware and flexible software. In this prototype, they used the hosts to set parameter and exchange data. Together with this, they employed the universal software radio peripherals (USRPs) to process baseband and radio frequency (RF) signals, as well as implemented the RIS to transmit and receive signals. Reference [23] studied a mmWave system relying on several RIS arrays which implemented low-precision analog-to-digital converters (ADCs). To assist multiple-input multiple-output (MIMO) transmission, these RIS arrays form a synthetic channel with increased spatial diversity and power gain by enabling the linear spatial processing.

1.1. Related Work. The authors in [26] investigated system performance of NOMA-RIS characterizing the effective channel gains corresponding with the best case and worst case of new channel statistics. They derived the closed-form formulas corresponding to the best case and worst case to examine two main system performance metrics such as the outage probability, the ergodic rate. For providing further insights, they also studied both the diversity orders of the outage probability and the ergodic rate at high signal-to-noise (SNR) region. In [27], a multiple-input multiple-output (MIMO) scheme along with passive beam forming weight are required to implemented NOMA-RIS systems which simultaneously serve groups of two users. The authors concluded that by enabling large number of RIS elements, the intercluster interference can be eliminated. Reference [28] introduced a system model of system with rate splitting multiple access- (RSMA-) aided RIS. Considering the phase shifts of the RIS and beam forming of the base station, the authors presented optimal policy in terms of energy efficiency.

However, a few paper considered advantage of RIS systems relying on NOMA, and most of the derivations are still complicated. Once can recognize different performance between RIS-NOMA and RIS-OMA, users' fairness along with their outage performance are not still studied in detail. Therefore, references [26–28] motivate us to investigate system performance metric for RIS-aided NOMA systems.

The main contributions of this paper are as follows

(i) Different from [29–32], this paper presents a RIS-aided NOMA system in down link to achieve benefits from NOMA to communicate simultaneously with their corresponding destinations via a RIS. It is assumed that the LIS is in the form of a reflect-array comprising N simple and reconfigurable reflector elements and controlled by a communication-oriented software. Unlike other published work dealing with the calculation of symbol error probability (SEP), our work provides outage performance evaluation of the RIS-aided NOMA system in the presence of hardware impairments

(ii) The closed-form expressions of outage probability for the RIS-aided NOMA system are derived. Since they are formulated in terms of various system parameters, the effect of each system parameter on the outage probability can be numerically evaluated. For instance, the effect of the number of metasurfaces in RIS on the outage probability can be evaluated to how the system can improve its performance in practice. It is demonstrated in this work that the outage probability of the system mainly relying on the number of metasurfaces in RIS

(iii) The derivations of asymptotic outage probabilities at high transmit signal-to-noise ratio (SNR) for two users are also provided as an important evaluation to design such the RIS-aided NOMA system in practice. Furthermore, compared with orthogonal multiple access- (OMA-) assisted RIS system, the considered system exhibits more benefits, and it becomes a prominent candidate to implement for forthcoming networks

2. System Model

We consider two-user approach of NOMA downlink relying on RIS to serve dedicated groups of NOMA users, as scheme 1 which is shown in Figure 1. It is reasonable to study two users which are expected acceptable performance. In fact, there are many groups of users which are normally separated by orthogonal access manner. In each group, we assume the representative users including near user (NU) and far user (FU) which are classified based on their locations. In this circumstance, one could not be transmission from the base station (BS) to mobile users directly due to heavy blockage or obstacle. The BS generates two beamforming vectors together with technique of zero forcing beamforming to serve two NOMA users. By grouping of paired users, RIS-NOMA satisfies different QoS requirements which are suitable to develop multiple services for mobile users in future wireless systems. In addition, considering the case of RIS equipped N reflecting elements which cannot serve FU. This

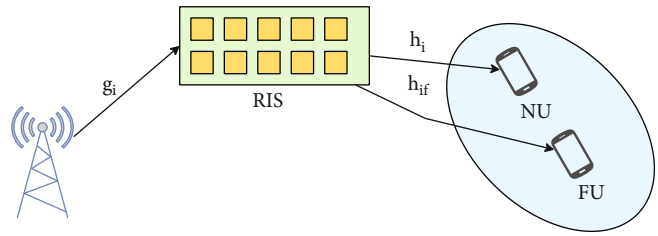

Figure 1: Scheme 1: NOMA-RIS System without direct link.

is reported as scheme 2, in which user U_3 just communicates with the BS, but user U_3 still be paired with user U_1. It is worth noting that U_1 belongs to link BS-RIS-destination. In scheme 2, the RIS has challenged once not only cannot reach to user U_3but also suffers interference from non-NOMA user.

Regarding operation of RIS, it is also equipped with a controller associated with switching procedure including working modes. RIS operate in receiving mode for channel estimation and in reflecting mode for data transmission. Since the RIS is a passive reflecting equipment, we adopt a time-division duplexing (TDD) protocol for uplink and downlink transmissions and assume channel reciprocity for achieving the channel information acquisition in the downlink based on the uplink training sequence. (To enable NOMA scheme in RIS-aided systems, user grouping must be achieved firstly; at the receiving end, we cannot guarantee similar quality of service for users. Therefore, by grouping user's fairness is the main benefit from deployment of NOMA. To guarantee the fairness and system performance, two-user model is adopted which is enough to benefit NOMA to RIS-assisted applications. In case of more users in a group, the worst performance occurs at several users. However, explicit mathematical analysis is also provided in a framework as [29].)

To enable NOMA mode, the superimposed signal $(a_1 s_1 + a_2 s_2)$ transmitted from the BS then is required to serve distant mobile users with the presence of RIS. This study considers NOMA concept to provide user fairness with a_1 and a_2 that are power allocation factors for user NU, and FU, respectively. Due to less amount of power required to supply for user NU, we have $a_1 < a_2$ and $a_1^2 + a_2^2 = 1$. To easy present other steps of signal analysis, we denote main parameters as Table 1.

In particular, the received signals at user NU and user FU are given, respectively, by

$$y_{\mathrm{NU}} = h_N^H \Theta_N G w (a_1 s_1 + a_2 s_2) + n_N, \tag{1}$$

$$y_{\mathrm{FU}} = h_F^H \Theta_F G w (a_1 s_1 + a_2 s_2) + n_F, \tag{2}$$

where G is denoted as the complex Gaussian channel matrix form $N \times 1$ which is transmitted from the BS to the RIS to reflect signal to distant users, n_N and n_F are noise terms, and h_N and h_F represent the complex Gaussian channel vector terms for links RIS-NU and RIS-FU, respectively. It can expand N as where P and Q are integers. The matrix$\Theta_u (u = N, F)$contains its diagonal elements $\beta_u \exp(-j\theta_{u,i})$with$\beta_N$as the amplitude reflection factor while $\theta_{N,i}$stands for the reflection phase shift. We limit our consideration on small scale fading. It is noted that G and h_u follow independent complex Gaussian distribution with zero mean and unit variance. (`The channel state information (CSI) regarding channels G and $h_u$is assumed to be available via the channel estimation approaches in the literature such as work in [33]. It is assumed that the RIS is associated with a reliable control channels, and hence the information about the predetermined beamforming vectors w can be sent to the users the FU and the NU.)

We call $D_u$as a diagonal matrix with its diagonal elements obtained from h_u^H, and V is an N×1 vector which includes the elements on the main diagonal of Θ_u^H. Then, by denoting $A = |v_p^H D_N h_N|$, we can compute some main equations as follows. We can compute the signal to interference plus noise (SINR) for the user NU to decode the FU's signal that is expressed by [29].

$$\mathrm{SINR}(s_2) = \max_{V_P} \frac{A^2 a_2^2}{A^2 a_1^2 + (1/\rho)}, \tag{3}$$

where ρ represents the transmit signal-to-noise ratio (SNR). By performing SIC, the user NU eliminates signal s_2, and then it decodes its signal by computing SNR as

$$\mathrm{SNR}(s_1) = \max_{V_P} A^2 a_1^2 \rho. \tag{4}$$

Before computing SINR to detect the FU's signal, we should denote new variable, i.e., $B = |v_p^H D_F h_F|$. Then, such SINR is given by

$$\mathrm{SINR}_{\mathrm{FU}} = \max_{V_P} \frac{B^2 a_2^2}{B^2 a_1^2 + (1/\rho)}. \tag{5}$$

Remark 1. It is noted that the expressions of SINR or SNR are main factor to evaluate system performance, for example, in (3)–(5), and imply that these factors depend on the SNR at the BS is ρ. Furthermore, we note that the SINR formulas include the products of the complex Gaussian distributed random variables, i.e., A and B, which lead to more complicated computations for RIS-NOMA if we need evaluate other metrics.

Table 1: Main parameters and denotations.

Parameter	Explanation
ρ	Signal-to-noise ratio at the BS
N	The number of RIS elements
a_1	Power allocation coefficient for signal s_1
a_2	Power allocation coefficient for signal s_2
R_1	Target rate of user NU
R_2	Target rate of user FU
$K_n(.)$	Bessel function of second kind
$\Gamma(.)$	Gamma function

3. Performance Analysis Scheme 1

In this section, we analyze the achievable performance of the proposed RIS-NOMA system in some scenarios, and benchmark scheme is also mentioned in Figure 2. It should be pointed out that as there are different decoding conditions for users NU and FU, we should compare performance gap among NU and FU, so that the main parameters are decided to guarantee the fairness. For simplifying the system performance analysis on performance gap among two users, this paper just focuses on main performance metric, i.e., outage probability. Of course, the other system performance metrics of such networks will be further studied but it needs change to other method of computation. However, this study exhibits explicit performance metric and more accuracy formulas if we compare them with the conventional method which is also used to present the outage performance, namely, the central limit theorem (CLT), in which variables A and B are approximated as a Gaussian random variable with fixed mean values and variances. Outage probability is defined as ability of SINR less than the predefined SINR thresholds. Since more complicated computations regarding RIS which is the form of a reflect-array comprising$N$simple and reconfigurable reflector elements, and more matrix variables in computations, unlike other published work dealing with the calculation of symbol error probability (SEP) [34], our work focuses on main metric, i.e., outage performance evaluation of the RIS-aided NOMA system [35] to determine which scenario exhibiting better performance.

By denoting Pr (.) as outage probability, we can formulate such outage probability as

$$P_{\text{out}} = \Pr\left(\psi \le \rho_{\text{th}}\right), \tag{6}$$

where ψ is either SINR or SNR, and ρ_{th} is denoted as SINR/SNR threshold.

3.1. Channel Distribution. We put our attention on the probability density function (PDF) of the product of channels, for example, $\sqrt{Q}v_p^H D_N h_N$ corresponding to the user NU. Since the structure of$v_p,\sqrt{Q}v_p^H D_N h_N$, is considered as an inner product of two$Q\times 1$ complex Gaussian vector, it is worth noting that $v_p,\sqrt{Q}v_p^H D_N h_N$, is a complex Gaussian random variable with zero mean and variance$|h_N|^2$. More importantly, we have $|h_N|^2$ following gamma distribution. Therefore, the PDF of $\sqrt{Q}v_p^H D_N h_N$ can be obtained as follows [29].

$$f_{A^2}(x) = \frac{2x^{Q-1/2}}{\Gamma(Q)} K_{Q-1}\left(2\sqrt{x}\right). \tag{7}$$

3.2. Outage Probability at User NU. The outage behavior happens at the user NU once it fails to detect the FU's signal s_2 as well as its own signal s_1.

$$P_{\text{NU}} = P_{\text{NU},s_1} \times P_{\text{NU},s_2}, \tag{8}$$

where P_{NU,s_1} and P_{NU,s_2} are probability related to detecting signal s_1 and s_2, respectively. These expressions are determined based on required target rates R_1 and R_2 for users NU and FU, respectively.

In particular, the outage probability to user NU detect signal s_1 is given by

$$P_{\text{NU},s_1} = \Pr\left(\log\left(1 + \text{SINR}(\text{s}_1)\right) < R_1\right). \tag{9}$$

Similarly, the outage probability to user NU detect signal s_2 is given by

$$P_{\text{NU},s_2} = \Pr\left(\log\left(1 + \text{SINR}(\text{s}_2)\right) < R_2\right). \tag{10}$$

Proposition 2. *The outage probability for user NU is given below, where* $\psi = Q/\rho a_1^2$,

$$\psi_1 = \frac{Q\epsilon_1}{\rho\left(a_2^2 - a_1^2\epsilon_1\right)}, \epsilon_1 = 2^{R_1} - 1, C_1 = \frac{1}{\Gamma(Q)^P}\psi^{\frac{P(Q-1)}{2}}, C_2 = \frac{1}{\Gamma(Q)^P}\psi_1^{\frac{P(Q-1)}{2}}, B_1 = K_Q\left(2(\psi)^{\frac{1}{2}}\right) \text{ and } B_2 = K_Q\left(2(\psi_1)^{\frac{1}{2}}\right),$$

$$P_{NU} = C_1 C_2\left[(\psi\psi_1)^{-\frac{Q+1}{2}}(\Gamma(Q))^2 - 2\psi^{-\frac{Q+1}{2}}\Gamma(Q) - 2\psi_1^{-\frac{Q+1}{2}}\Gamma(Q) + 4\psi^{-\frac{1}{2}}\psi_1^{-\frac{1}{2}}B_1B_2\right]^P. \tag{11}$$

Proof. See in Appendix A. □

3.3. Outage Probability at User FU

Proposition 3. *The outage probability for user FU is given as [12], where* $\psi_2 = Q\epsilon_2/\rho(a_2^2 - a_1^2\epsilon_2)$, $\epsilon_2 = 2^{R_2} - 1$, $C_3 = (1/\Gamma(Q)^P)\psi_2^{P(Q-1)/2}$, *and* $B_3 = K_Q(2(\psi_2)^{1/2})$.

$$P_{FU} = C_3\left((\psi_2)^{-\frac{Q+1}{2}}\Gamma(Q) - 2(\psi_2)^{-\frac{1}{2}}B_3\right)^P. \tag{12}$$

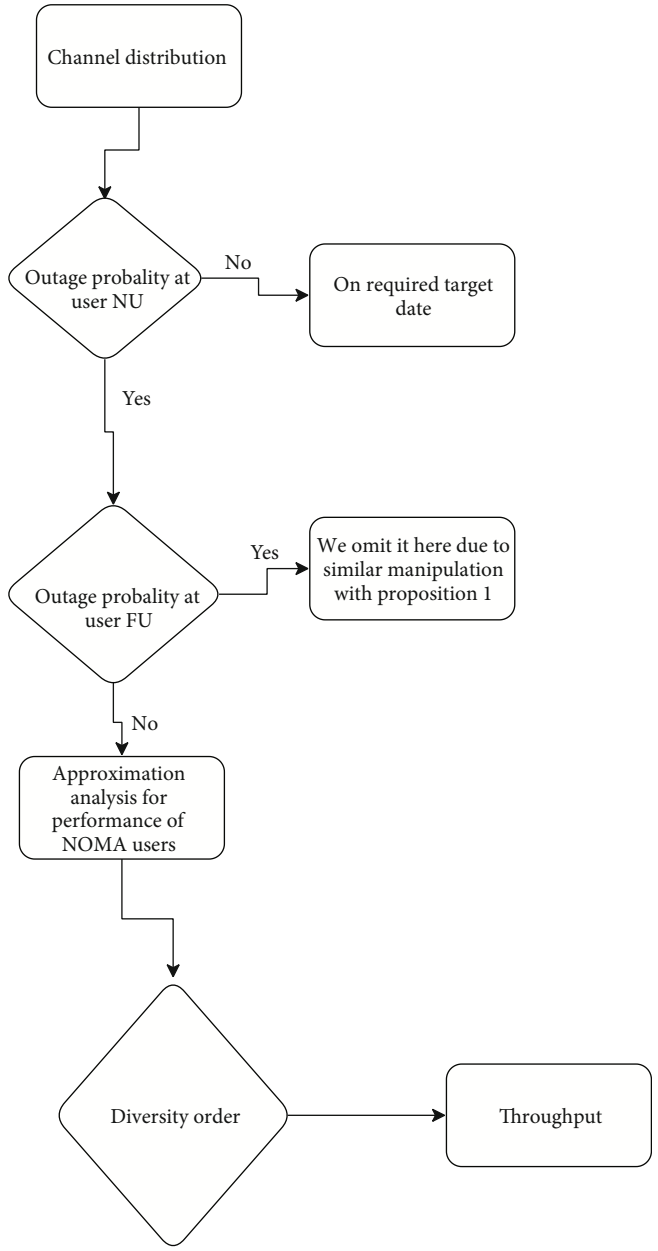

Figure 2: Flowchart for methodology.

Proof. We omit it here due to similar manipulations with Proposition 2. □

3.4. Approximation Analysis for Performance of NOMA Users. To look at insights of the considered system, the approximation computations are necessary to determine outage behavior in simpler manner. In particular, at high SNR regime, we have two cases.

(i) Case 1.

If $Q > 1$ and $n \geq 2$, we can follow $K_Q(z) \approx 1/2((n-1)!/(z/2)^n - (n-2)!/(z/2)^{n-2})$ to achieve valued computation. Precisely, the approximated outage probability of two NOMA users can be obtained as below.

$$P_{NU,s_1}^{\infty} = \frac{\psi^p}{(Q-1)^p}, P_{NU,s_2}^{\infty} = \frac{{\psi_1}^p}{(Q-1)^p}, \tag{13}$$

$$P_{FU,1}^{\infty} = \frac{\left(Q\epsilon_2/\rho\left(a_2^2 - a_1^2\epsilon_2\right)\right)^p}{(Q-1)^p}. \tag{14}$$

(ii) Case 2.

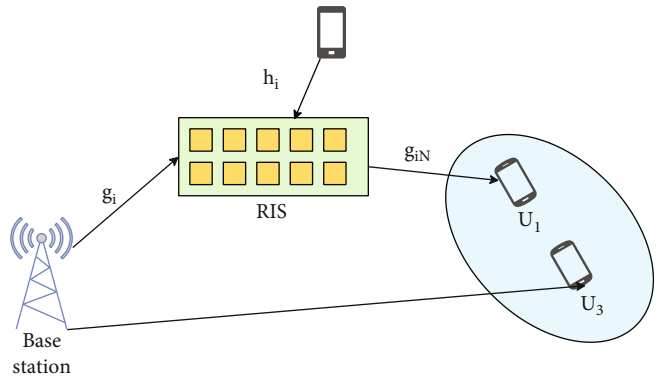

Figure 3: Scheme 2: NOMA-RIS System with direct link.

Table 2: Simulation parameters.

Description	Parameter
Power allocation coefficient	$a_1 = 0.2$ and $a_2 = 0.8$
Relative Channel estimation error	$\eta_k = 1 \times 10^{-4} \sim 9 \times 10^{-4}$
NOMA user corresponding two cases	$Q > 1$ and $Q = 1$
Distance between two nodes	$d_{SU_1} = 0.04$, $d_{SR} = 0.06$ $d_{RU_1} = 0.02$, $d_{SU_2} = 0.04$ $d_{U_1U_2} = 1 - d_{SU_1}$
Transmit SNR	$\rho = 0 \sim 30$dB
Target rates	$R_1 = 1$ BPCU, $R_2 = 1$ 1 BPCU, and $R_{OMA} = 1$ (BPCU)

Especially, at high SNR and $Q = 1$, we have $K_1(z) = 1/2\,(1/(z/2)) + (z/2)In(z/2)$; the approximated result of outage probability for two users are written as

$$P_{NU,s_1}^{\infty,2} = \psi^N\left(-\ln(\psi)^N\right), P_{NU,s_2}^{\infty,2} = {\psi_1}^N\left(-\ln(\psi_1)^N\right), \quad (15)$$

$$P_{FU,2}^{\infty,2} = \left(\frac{Q\epsilon_2}{\left(\rho\left(a_2^2 - a_1^2\epsilon_2\right)\right)}\right)^N \left(-\ln\left(\frac{Q\epsilon_2}{\left(\rho\left(a_2^2 - a_1^2\epsilon_2\right)\right)}\right)\right)^N. \quad (16)$$

3.5. Diversity Order. To further evaluate performance of two users in case of high SNR, it needs to consider the diversity order for the case Q = 1. In particular, such diversity order metrics can be formulated by [35].

$$D_{NU} = \lim_{\rho \longrightarrow \infty} \left(\frac{\log(P_{NU})}{\log \rho}\right) = \lim_{\psi_1 \longrightarrow \infty} \left(\frac{\log(P_{NU})}{\log \psi_1}\right) = N^2, \quad (17)$$

$$D_{FU} = \lim_{\rho \longrightarrow \infty} \left(\frac{\log(P_{FU})}{\log \rho}\right) = \lim_{\psi_2 \longrightarrow \infty} \left(\frac{\log(P_{FU})}{\log \psi_2}\right) = N. \quad (18)$$

Remark 4. Since (17) and (18) show that the number of reflecting elements in RIS decides how the system performance can be improved, once we enhance the main parameter SNR at the BS, in the next section of numerical simulation, it is predicted that the curves of outage probability will be reduced sharply at high value of N.

3.6. Throughput. In delay-limited transmission mode, more system metric, namely, throughput is decided by fixed data rates R_1 and R_2 and achieved outage probability in the previous section. Therefore, the throughput of the whole system is expressed by [35]

$$T = R_1(1 - P_{NU}) + R_2(1 - P_{FU}). \quad (19)$$

Further, such throughput is rewritten as

$$T = R_1\left(1 - \left(P_{NU,s_1}\right) \times \left(P_{NU,s_2}\right)\right) + R_2(1 - P_{FU}). \quad (20)$$

4. Scheme 2: RIS-NOMA System with Direct Link

As Scheme 2 was shown in Figure 3, it is challenging once user U_3 just relies on direct link associated with the BS. Assuming that the corresponding channel h between user$U_3$and the BS follows Rayleigh fading, it is worth noting that RIS still communicates with userU_1while it has interference from external non-NOMA user. In this circumstance, the BS sends signal $(a_1s_1 + a_3s_3)$ with conditions $a_1 + a_3 = 1, a_3 > a_1$ to two users, U_1 and U_3. In the first time slot, user U_1detects U_3's signal and then detects its own signal. In the contrast, user only detects its signal since user U_3 prioritizes to detect signal (more power allocated to user U_3 for such priority $a_3 > a_1$). In particular, the received signals at user U_1 and user U_3 are given, respectively, by

$$y_{U_1} = g_N^H \Theta_N G w(a_1s_1 + a_2s_2) + n_I + n_{U_1}, \quad (21)$$

$$y_{U_3} = h(a_1s_1 + a_2s_2) + n_{U_3}, \quad (22)$$

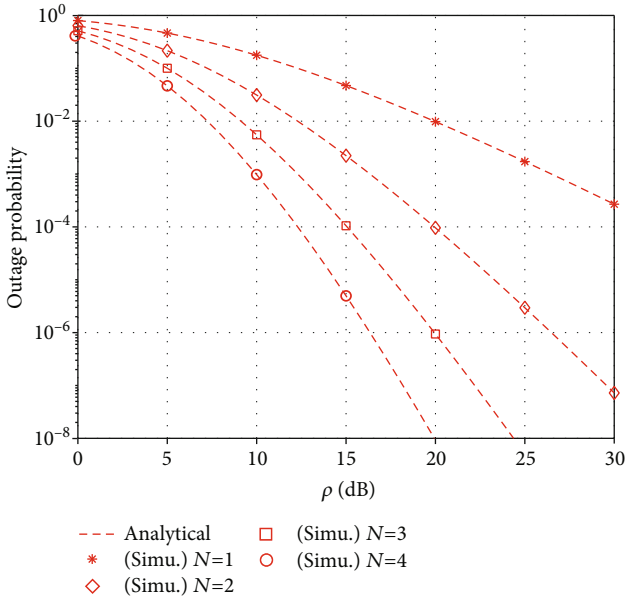

Figure 4: Outage probability of user NU versus the transmit SNR ($Q = 1$).

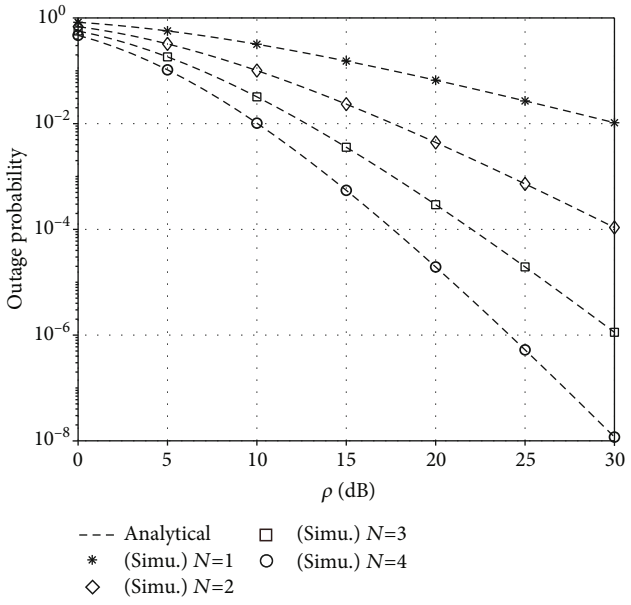

Figure 5: Outage probability for NOMA FU ($Q = 1$).

where n_I is interference term from normal user; n_{U_1}, n_{U_3} are AWGN noise terms. By exploiting the central limit theorem (3.9.2) in [36], all interference signals from external sources can be treated as AWGN noise with $\mathrm{CN}(0, \Omega_1)$.

To proceed signal detection, SINRs can be obtained at user U_1 and U_3, respectively,

$$\mathrm{SINR}_{U_1} = \max_{V_P} \frac{a_1^2 A^2}{h_I + (1/\rho)}, \tag{23}$$

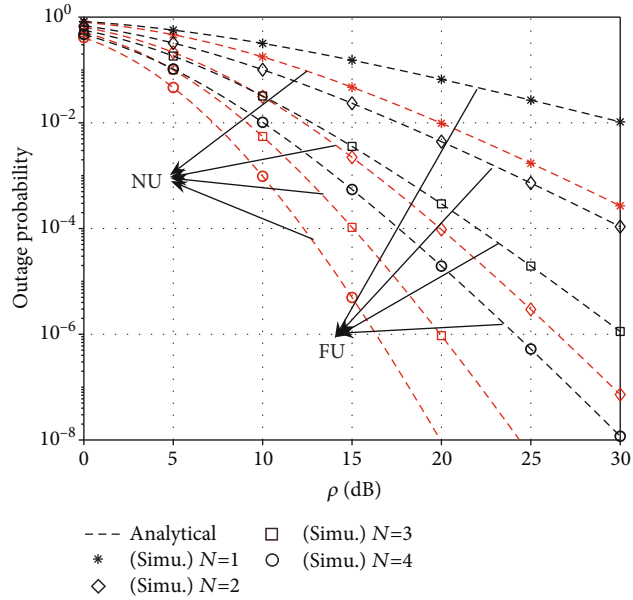

Figure 6: Outage probability comparison for users NU and FU.

$$\mathrm{SINR}_{U_1} = \frac{a_3^2 \rho(h)^2}{a_1^2 \rho(h)^2 + 1}. \tag{24}$$

The outage probability for user U_1 is similar as user NU in scheme 1, and we do not want to replica it in this section. It is noted that the degraded performance is resulted by coefficient Ω_1.

Since channel h follows Rayleigh fading with mean of λ_h, the outage probability of user U_3 is given as

$$P_{U_3} = 1 - e^{\frac{\epsilon_1 \lambda_h}{2\left(a_2^2 - a_1^2 \epsilon_2\right)\rho}}. \tag{25}$$

5. Benchmark Scheme: OMA

In the context of OMA, only single signal is transmitted from the BS to each user. As a result, SNR at the destination associated with the link containing RIS is given by

$$\mathrm{SNR}_{\mathrm{OMA}} = \max_{V_P} \mathrm{A}^2 \rho. \tag{26}$$

Proposition 5. *The outage probability of user in the RIS-aided system relying on OMA scheme is given as*

$$P_{OMA} = \frac{1}{\Gamma(Q)^P} \psi_4^{\frac{P(Q+1)}{2}} \left(\psi_4^{-\frac{P(Q+1)}{2}} \Gamma(Q) - 2\psi_4^{-\frac{1}{2}} K_Q\left(2\psi_4^{-\frac{1}{2}}\right)\right)^P, \tag{27}$$

where $\psi_4 = Q\epsilon_{OMA}/\rho$ *and* $\epsilon_{OMA} = 2^{2R_{OMA}} - 1$.

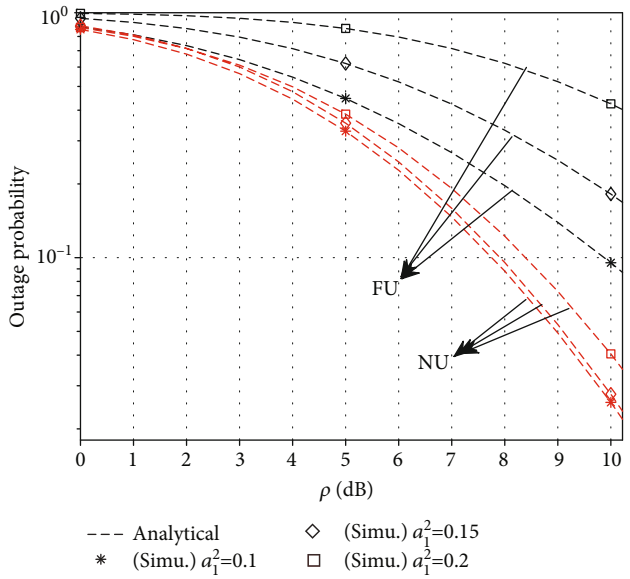

Figure 7: Outage probability comparison for users NU and FU with different power allocation factors ($N = 4$).

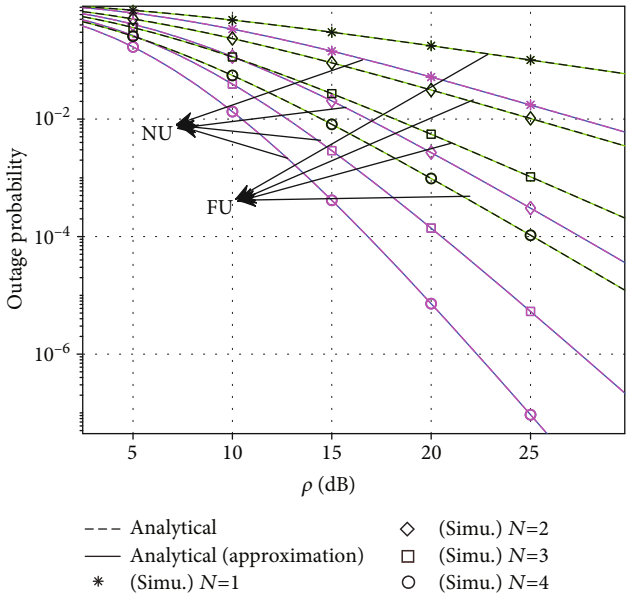

Figure 8: Outage probability comparison between NOMA and NOMA-approximation ($Q = 2$).

Similarly, we also obtain approximated computation for OMA user corresponding to two cases $Q > 1$ and $Q = 1$, respectively, as

$$P_{OMA,1}^{\infty} \approx \frac{\psi_4}{(Q-1)^P}, \tag{28}$$

$$P_{OMA,2}^{\infty} \approx \psi_4^N (-\ln(\psi_4))^N. \tag{29}$$

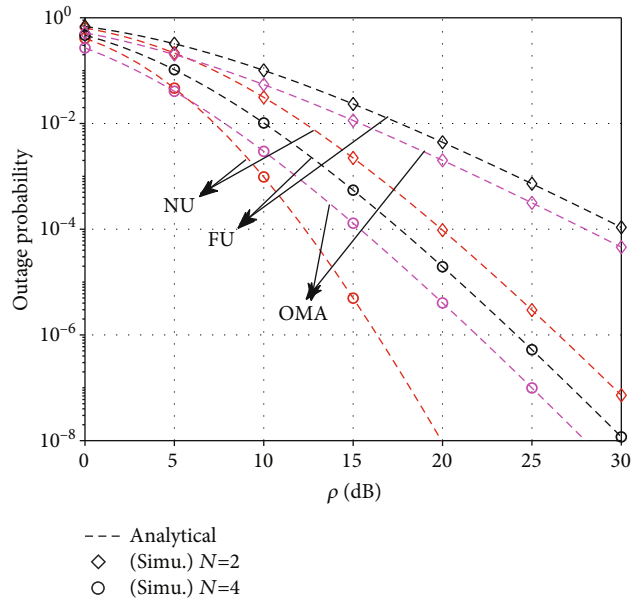

Figure 9: Outage probability comparison between RIS relies on NOMA and OMA ($Q = 1$).

6. Numerical Simulations and Discussions

In this section, we will determine system performance metrics (outage probability and throughput in delay-limited transmission mode). We intend to verify the theoretical results, numerically evaluate, and compare two practical schemes of the RIS-NOMA system. In each figure, we can see the main parameters used for simulation. We call bit per channel use as BPCU for short. We set target rate $R_1 = 1$ (BPCU), $R_2 = 1$ (BPCU), and $R_{\text{OMA}} = 1$ (BPCU) and power allocation factors $a_1^2 = 0.2, a_2^2 = 1 - a_1^2$, except for specific cases indicated later, and simulation parameters used are summarized in Table 2.

Figure 4 shows the outage probability versus transmit SNR at the BS. It can be seen intuitively that the simulation and analytical results are matched very tight. In this graph, it mainly shows how two NOMA groups can make the exchange of the messages between each other. The improvements which are shown over here are mainly regarding the performance of the outage and here the things which are mainly considered are about the SNR. We consider the improvement of outage performance for different numbers of RIS elements for user NU in the range of SNR (from 0 to 30 dB). In particular, the significant improvement can be achieved at ρ equals to 30 dB. It can be observed that when the number of RIS elements increase, the performance of the proposed RIS-NOMA system exhibits its efficiency as expected from our study. Since diversity order depends on the number of metasurfaces N, once can see that significant improvement of outage probability occurs if N increases.

Similarly, since computation of outage probability for user FU is simpler than that of user NU, performance of Figure 4 is similar. Figure 5 shows the trends of outage probability versus transmit SNR. The main purpose of this graph

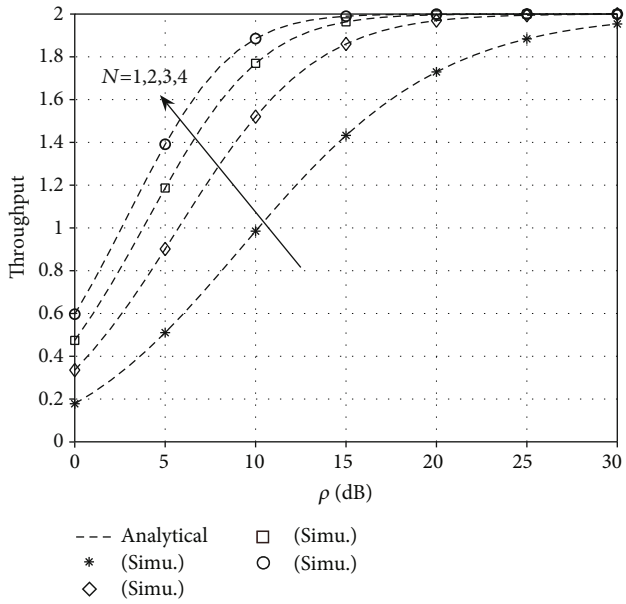

Figure 10: Throughput of the RIS-NOMA system ($Q = 1$).

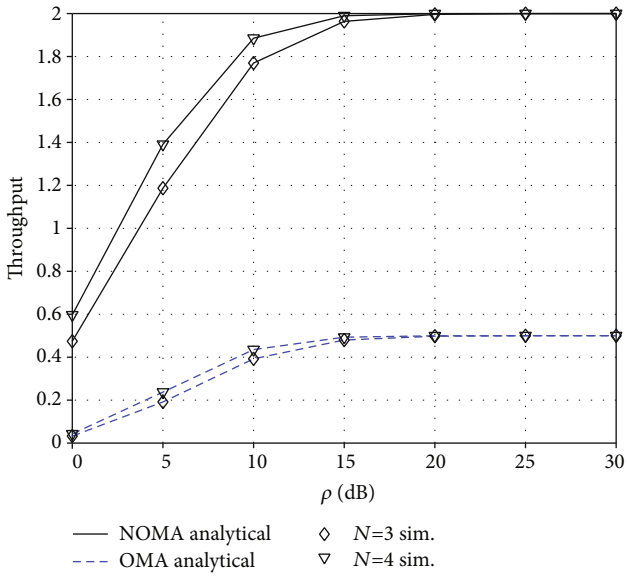

Figure 11: Throughput comparison between RIS-NOMA and RIS-OMA system ($Q = 1$).

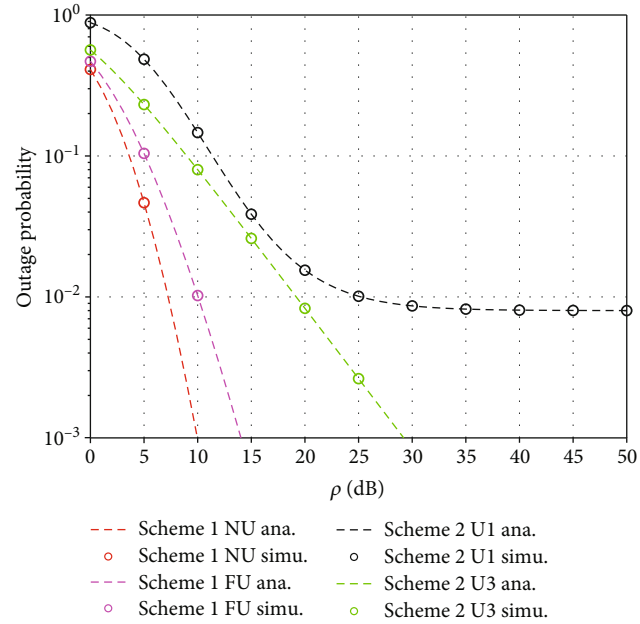

Figure 12: Outage probability comparison for Scheme 1 and Scheme 2, $Q = 1$, $N = 4$, and $\Omega_I = 0.03$.

is to show the performance of the users which is very important to be understood in order to determine various benefits. Here also, we can observe that the performance of the proposed RIS-NOMA benefits to user at far distance by increasing the number the RIS elements and higher power assigned to user FU.

Figure 6 shows the comparison of the outage probability versus SNR for different numbers of RIS elements for users NU and FU. In this comparison, we can determine that as the RIS elements are increased, the performance of the NU is better that of the FU. It seems that RIS elements which are there used have a great proficiency in case of maintaining performance rate. The rate of the determination that is done over here is related to mainly increase rate of the performance. However, it is more complicated processing at user NU compared with that in user FU.

Here, it can be seen from Figure 7 that the comparison is mainly done between NU and FU where the power allocation is shown where $N = 4$. The comparison which is done over here is related to the outage-based probability.

Figure 7 demonstrates the impact of power allocation factors on the outage probability. Since expression of outage probability for user NU depends on ability of detecting user FU's signal, lower factor a_1 results in better performance for user NU. As previous simulations, we can see similar trends of such outage performance in this figure, while Figure 8 indicates that exact and approximated formulas for two users have similar performance. For simple computation, we also benefit similar result. Here, mainly the outage comparison which is done is between the NOMA and NOMA approximation, it is very important to find the difference between the two NOMA in order to fund the trend to be identified.

Figure 9 indicates the comparison of the outage performance for users NU, FU in NOMA scheme, and user in OMA scheme. It can be observed that the outage behavior of user NU is better than OMA user and user FU. The main reason is that different power factors and signal detecting procedure lead to performance gaps. The importance of the RIS lies within the NOMA which is understood with the help of the comparison between NOMA and NOMA with the use of $Q = 1$.

Figure 10 depicts throughput performance versus transmit SNR. It can be concluded that more elements of RIS lead to higher throughput. The main reason is that the

throughput depends on the outage probability while higher number of RIS elements results in better outage performance. The ceiling value of such throughput can be achieved at the point $\rho = 20dB, N = 4$. Two target rates R_1 and R_2 make this ceiling value. The main things which are been depicted here is related to the RIS-NOMA system which shows the rate of activity that is taking place.

The comparison throughput performance for the considered system with OMA is shown in Figure 11, when ρ is raised. We set $R_1 = R_2 = 1$ in this case. This suggests that our system can approach two at a very high ρ value. It is easy to see how such throughput is influenced by the outage probabilities attained in earlier steps. It has been confirmed that our RIS system based on NOMA is superior to that based on OMA.

Figure 12 shows the comparison of the outage probability versus SNR for NOMA-RIS system in two schemes. It can be seen clearly that scheme 1 shows better outage performance compared with that in scheme 2. It is suitable with analytical results once scheme 2 has less benefit from fabrication of RIS. Furthermore, interference from external non-NOMA user limits performance of user U_1 which has similar configuration with user NU in scheme 1. The value regarding the scheme 1 and the scheme 2 has been shown over here which is a value of the external non-NOMA user limits. It is found that all the results which are given are suitable with the limits.

7. Conclusions

In this paper, we study two practical situations for deployment of RIS and NOMA in wireless system. More RIS elements lead to significant improvement in main system metric, i.e., outage probability. In particular, we derived the closed form formulas of outage probability which depend on various parameters such as the number of RIS elements, transmit SNR at the BS, and power allocation factors. By controlling these values, we can achieve reasonable system performance. The numerical results also indicate that the RIS-NOMA in scheme 1 is reported as better case. However, to achieve such ideal performance, it is necessary to release the impact of interference to the RIS. By exploiting NOMA, the RIS-NOMA aided system provides better performance compared with traditional multiple access techniques such as OMA. In addition, by grouping of users, we benefit advantages of NOMA while separating these groups by employing OMA scheme. Therefore, such RIS-NOMA becomes promising system for many applications in wireless systems, especially massive connections is strictly required in future systems.

Appendix

A. Proof of Proposition 2.

The outage probability P_{NU,s_1} can be further computed by

$$P_{\mathrm{NU},s_1} = \int_0^{\psi} f_{A^2}(x)dx. \tag{A.1}$$

From achieved PDF, we then calculate such outage probability as below:

$$P_{\mathrm{NU},s_1} = \int_0^{\psi} \frac{2x^{\mathrm{Q}-1/2}}{\Gamma(Q)} K_{Q-1}\left(2\sqrt{x}\right)dx. \tag{A.2}$$

In the next step, P_{NU,s_1} can be given by

$$P_{\mathrm{NU},s_1} = C_1\left((\psi)^{-\frac{Q+1}{2}}\Gamma(Q) - 2(\psi)^{-\frac{1}{2}}B_1\right)^P. \tag{A.3}$$

Regarding signal processing at the NU, this user needs detect the FU's signal since the NU treats the FU's signal as noise. The outage probability of the NU depends partly on ability of detecting the FU's signal as below:

$$P_{\mathrm{NU},s_2} = \Pr\left(\log\left(1 + \mathrm{SINR}(s_2)\right) < R_2\right). \tag{A.4}$$

Then, P_{NU,s_2} can be rewritten by

$$P_{\mathrm{NU},s_2} = C_2\left((\psi_1)^{-\frac{Q+1}{2}}\Gamma(Q) - 2(\psi_1)^{-\frac{1}{2}}B_2\right)^P. \tag{A.5}$$

It is noted that the outage probability for user NU is decided by two mentioned steps, and then we have such outage probability as

$$P_{\mathrm{NU}} = P_{\mathrm{NU},s_1} \times P_{\mathrm{NU},s_2}. \tag{A.6}$$

Next, we can obtain such outage probability for user NU as [(A.8)]

$$P_{\mathrm{NU}} = C_1\left(\psi^{-\frac{Q+1}{2}}\Gamma(Q) - 2\psi^{-\frac{1}{2}}B_1\right)^P \times C_2\left({\psi_1}^{-\frac{Q+1}{2}}\Gamma(Q) - 2{\psi_1}^{-\frac{1}{2}}B_2\right)^P, \tag{A.7}$$

$$\begin{aligned} P_{\mathrm{NU}} = C_1C_2\Big[&(\psi\psi_1)^{-\frac{Q+1}{2}}\Gamma(Q)^2 - 2\psi^{-\frac{Q+1}{2}}{\psi_1}^{-\frac{1}{2}}B_2\Gamma(Q) \\ &- 2\psi^{-\frac{Q+1}{2}}{\psi_1}^{-\frac{1}{2}}B_1\Gamma(Q) + 4\psi^{-\frac{1}{2}}{\psi_1}^{-\frac{1}{2}}B_1B_2\Big]. \end{aligned} \tag{A.8}$$

This completes the proof.

B. Proof of Proposition 5.

Similarly, since we have PDF of A is given by

$$\mathrm{f}_{\mathrm{A}^2}(\mathrm{x}) = \frac{2\mathrm{x}^{\mathrm{Q}-1/2}}{\Gamma(\mathrm{Q})}\mathrm{K}_{\mathrm{Q}-1}\left(2\sqrt{\mathrm{x}}\right). \tag{A.9}$$

The outage probability of OMA user can be expressed by

$$P_{\mathrm{OMA}} = \Pr\left(\log\left(1 + \mathrm{SINR}_{\mathrm{OMA}}\right) < R_{\mathrm{OMA}}\right), \tag{A.10}$$

where R_{OMA} is target rate for OMA user.
Next, P_{OMA} is computed by

$$P_{\mathrm{OMA}} = \frac{2}{\Gamma(Q)}\int_0^{\psi_4} x^{\frac{Q-1}{2}}K_{Q-1}\left(2\sqrt{x}\right)dx. \tag{A.11}$$

By apply similar manipulation as the case of NOMA, the final result can be obtained, and hence, the proof is completed.

Data Availability

No data were used to support this study.

Conflicts of Interest

The authors declare that they have no conflicts of interest.

References

[1] H. Huang, W. Xia, J. Xiong, J. Yang, G. Zheng, and X. Zhu, "Unsupervised learning-based fast beamforming design for downlink MIMO," *IEEE Access*, vol. 7, pp. 7599–7605, 2018.

[2] G. Gui, H. Sari, and E. Biglieri, "A new definition of fairness for non-orthogonal multiple access," *IEEE Communications Letters*, vol. 23, no. 7, pp. 1267–1271, 2019.

[3] B. Wang, F. Gao, S. Jin, H. Lin, and G. Y. Li, "Spatial- and frequency wideband effects in millimeter-wave massive MIMO systems," *IEEE Transactions on Signal Processing*, vol. 66, no. 13, pp. 3393–3406, 2018.

[4] H. Xie, F. Gao, S. Zhang, and S. Jin, "A unified transmission strategy for TDD/FDD massive MIMO systems with spatial basis expansion model," *IEEE Transactions on Vehicular Technology*, vol. 66, no. 4, pp. 3170–3184, 2017.

[5] Z. M. Fadlullah, F. Tang, B. Mao et al., "State-of-the-art deep learning: evolving machine intelligence toward tomorrow's intelligent network traffic control systems," *IEEE Communications Surveys & Tutorials*, vol. 19, no. 4, pp. 2432–2455, 2017.

[6] N. Kato, Z. M. Fadlullah, B. Mao et al., "The deep learning vision for heterogeneous network traffic control: proposal, challenges, and future perspective," *IEEE Wireless Communications*, vol. 24, no. 3, pp. 146–153, 2016.

[7] F. Tang, B. Mao, Z. M. Fadlullah, and N. Kato, "On a novel deep-learningbased intelligent partially overlapping channel assignment in SDN-IoT," *IEEE Communications Magazine*, vol. 56, no. 9, pp. 80–86, 2018.

[8] D.-T. Do and A.-T. Le, "NOMA based cognitive relaying: transceiver hardware impairments, relay selection policies and outage performance comparison," *Computer Communications*, vol. 146, pp. 144–154, 2019.

[9] T. Do, A.-T. Le, Y. Liu, and A. Jamalipour, "User grouping and energy harvesting in UAV-NOMA system with AF/DF relaying," *IEEE Transactions on Vehicular Technology*, vol. 70, no. 11, pp. 11855–11868, 2021.

[10] D.-T. Do, M.-S. Van Nguyen, T.-A. Hoang, and B. M. Lee, "Exploiting joint base station equipped multiple antenna and full-duplex D2D users in power domain division based multiple access networks," *Sensors*, vol. 19, no. 11, p. 2475, 2019.

[11] D.-T. Do, A.-T. Le, C.-B. Le, and B. M. Lee, "On exact outage and throughput performance of cognitive radio based non-orthogonal multiple access networks with and without D2D link," *Sensors*, vol. 19, no. 15, p. 3314, 2019.

[12] D.-T. Do, A.-T. Le, T. N. Nguyen, X. Li, and K. M. Rabie, "Joint Impacts of Imperfect CSI and Imperfect SIC in Cognitive Radio-Assisted NOMA-V2X Communications," *IEEE Access*, vol. 8, no. 7, pp. 128629–128645, 2020.

[13] D.-T. Do, A.-T. Le, and B. M. Lee, "NOMA in cooperative underlay cognitive radio networks under imperfect SIC," *IEEE Access*, vol. 8, pp. 86180–86195, 2020.

[14] D.-T. Do, M. V. Nguyen, F. Jameel, R. Jäntti, and I. S. Ansari, "Performance evaluation of relay-aided CR-NOMA for beyond 5G communications," *IEEE Access*, vol. 8, pp. 134838–134855, 2020.

[15] Y. Liang, R. Long, Q. Zhang, J. Chen, H. V. Cheng, and H. Guo, "Large intelligent surface/antennas (LISA): making reflective radios smart," *Journal of Communications and Information Networks*, vol. 4, no. 2, pp. 40–50, 2019.

[16] E. Basar, "Transmission through large intelligent surfaces: a new frontier in wireless communications," in *2019 European Conference on Networks and Communications (EuCNC)*, Valencia, Spain, 2019IEEE.

[17] Z. Tang, T. Hou, Y. Liu, J. Zhang, and C. Zhong, "A novel design of RIS for enhancing the physical layer security for RIS-aided NOMA networks," *IEEE Wireless Communications Letters*, vol. 10, no. 11, pp. 2398–2401, 2021.

[18] Q. Wu and R. Zhang, "Towards smart and reconfigurable environment: intelligent reflecting surface aided wireless network," *IEEE Communications Magazine*, vol. 58, no. 1, pp. 106–112, 2020.

[19] M. D. Renzo, M. Debbah, D. T. Phan-Huy et al., "Smart radio environments empowered by reconfigurable AI meta-surfaces: an idea whose time has come," *EURASIP Journal on Wireless Communications and Networking*, vol. 2019, no. 1, 2019.

[20] M. di Renzo and J. Song, "Reflection probability in wireless networks with metasurface-coated environmental objects: an approach based on random spatial processes," *EURASIP Journal on Wireless Communications and Networking*, vol. 2019, no. 1, 2019.

[21] G. C. Alexandropoulos and E. Vlachos, "A hardware architecture for reconfigurable intelligent surfaces with minimal active elements for explicit channel estimation," in *ICASSP 2020 - 2020 IEEE international conference on acoustics, speech and signal processing (ICASSP)*, pp. 9175–9179, Barcelona, Spain, 2020.

[22] L. Dai, B. Wang, M. Wang et al., "Reconfigurable intelligent surface-based wireless communications: antenna design, prototyping, and experimental results," *IEEE Access*, vol. 8, pp. 45913–45923, 2020.

[23] X. Yang, C. -K. Wen, and S. Jin, "MIMO detection for reconfigurable intelligent surface-assisted millimeter wave systems," *IEEE Journal on Selected Areas in Communications*, vol. 38, no. 8, pp. 1777–1792, 2020.

[24] H. Lu, Y. Zeng, S. Jin, and R. Zhang, "Enabling panoramic full-angle reflection via aerial intelligent reflecting surface," in *2020 IEEE International Conference on Communications Workshops (ICC Workshops)*, Dublin, Ireland, 2020IEEE.

[25] M. Di Renzo, F. H. Danufane, X. Xi, J. de Rosny, and S. Tretyakov, "Analytical modeling of the path-loss for reconfigurable intelligent surfaces–anomalous mirror or scatterer?," in *2020 IEEE 21st International Workshop on Signal Processing Advances in Wireless Communications (SPAWC)*, Atlanta, GA, USA, 2020.

[26] T. Hou, Y. Liu, Z. Song, X. Sun, Y. Chen, and L. Hanzo, "Reconfigurable intelligent surface aided NOMA networks," *IEEE Journal on Selected Areas in Communications*, vol. 38, no. 11, pp. 2575–2588, 2020.

[27] T. Hou, Y. Liu, Z. Song, X. Sun, and Y. Chen, "MIMO-NOMA networks relying on reconfigurable intelligent surface: a signal cancellation based design," *IEEE Transactions on Communications*, vol. 68, no. 11, pp. 6932–6944, 2020.

[28] Z. Yang, J. Shi, Z. Li, M. Chen, W. Xu, and M. Shikh-Bahaei, "Energy efficient rate splitting multiple access (RSMA) with reconfigurable intelligent surface," in *2020 IEEE International Conference on Communications Workshops (ICC Workshops)*, pp. 1–6, Dublin, Ireland, 2020.

[29] Z. Ding and H. Vincent Poor, "A simple design of IRS-NOMA transmission," *Communications letters*, vol. 24, no. 5, pp. 1119–1123, 2020.

[30] M. Zeng, W. Hao, O. A. Dobre, Z. Ding, and H. V. Poor, "Power minimization for multi-cell uplink NOMA with imperfect SIC," *IEEE Wireless Communications Letters*, vol. 9, no. 12, pp. 2030–2034, 2020.

[31] M. F. Hanif, Z. Ding, T. Ratnarajah, and G. K. Karagiannidis, "A minorization-maximization method for optimizing sum rate in the downlink of non-orthogonal multiple access systems," *IEEE Transactions on Signal Processing*, vol. 64, no. 1, pp. 76–88, 2016.

[32] Q. Chen, M. Li, X. Yang, R. Alturki, M. D. Alshehri, and F. Khan, "Impact of residual hardware impairment on the IoT secrecy performance of RIS-assisted NOMA networks," *IEEE Access*, vol. 9, pp. 42583–42592, 2021.

[33] Z. Wang, L. Liu, and S. Cui, "Channel estimation for intelligent reflecting surface assisted multiuser communications," in *2020 IEEE Wireless Communications and Networking Conference (WCNC)*, Seoul, Korea, 2020IEEE.

[34] Y. Liu and W.-K. Ma, "Symbol-level precoding is symbol-perturbed ZF when energy efficiency is sought," in *2018 IEEE International Conference on Acoustics, Speech and Signal Processing (ICASSP)*, pp. 3869–3873, Calgary, AB, Canada, 2018.

[35] A. Hemanth, K. Umamaheswari, A. C. Pogaku, D.-T. Do, and B. M. Lee, "Outage performance analysis of reconfigurable intelligent surfaces-aided NOMA under presence of hardware impairment," *IEEE Access*, vol. 8, pp. 212156–212165, 2020.

[36] T. Q. Quek, G. de la Roche, İ. Güvenç, and M. Kountouris, *Small Cell Networks: Deployment, PHY Techniques, and Resource Management*, Cambridge University Press, Cambridge, U.K., 2013.